GMR
The Original

COMPARATIVE STUDIES OF BIOETHANOL PRODUCTION FROM LIGNOCELLULOSIC FEEDSTOCKS FROM AGRICULTURAL WASTE

Praphulla Rao*[1], Prathibha Narayanan[1], Hadagali Ashoka[1], Tarun Mahesh[1], P Abhiram, Chandu R[1], Rohith Vasishta J[1]

[1]Department of Biotechnology, B.M.S. College of Engineering, Bull Temple Road, Bengaluru -560019, KA, India
*Corresponding author: praphullarao.bt@bmsce.ac.in

Received: 10th Dec, 2025; **Revised:** 15th Feb 2026**; Accepted:** 11th April, 2026; **Available Online:** 20th July, 2026

ABSTRACT
With the increasing global focus on climate change and the depletion of fossil fuels, bioethanol production has emerged as a promising alternative to traditional petroleum fuels. This study compares eight locally available lignocellulosic feedstocks including sugarcane bagasse, rice husk, maize husk, apple pomace, cassava peel, banana stem, jackfruit peel and cotton fibres, for bioethanol production using Saccharomyces cerevisiae. The experimental work investigates the impact of pre-treatment with $Ca(OH)_2$ for mitigating the inhibitory effects of furfural, which is a by-product of dilute acid hydrolysis pre-treatment. All the lignocellulosic feedstocks were evaluated for their ethanol yields, furfural content, and glucose utilisation under laboratory scale batch fermentation conditions. Among the feedstock sources, the maximum amount of ethanol was produced from rice husk (11.50 g/L), maize husk (11.54 g/L), and sugarcane bagasse (12.63 g/L). Apparent ethanol productivity values ranged between 0.282 g/L/day to 0.902 g/L/day with sugarcane bagasse showing highest productivity and furfural concentration was drastically reduced by 80.4%. This study was extended to 14 days to observe comparative insights on the suitability of the lignocellulosic feedstocks from agricultural waste residues, inhibitor reduction and laboratory scale process feasibility. Fourier Transform Infrared Spectroscopy (FTIR) qualitatively confirmed the presence of ethanol associated functional groups in all the distilled samples. The production of bioethanol in this study suggested predominantly non-growth associated product based on mathematical modelling.

KEYWORDS: Bioethanol, calcium hydroxide, furfural, second generation feedstocks, mathematical modelling

1. INTRODUCTION

Energy has played a major role in the development of the human race, driving economic and social growth. As the world population increases, energy needs continue to rise. Currently, fossil fuels provide most of the energy needs of the world. The burning of fossil fuels for energy has caused serious environmental problems, especially CO_2 emissions, on the planet in recent decades. Daily CO_2 and greenhouse gas emissions from fossil fuels are significant contributors to climate change [1]. According to NASA Earth Observatory and the IEA, the Global Carbon Budget states, daily CO_2 emissions from fossil fuels (coal, oil, and gas) total about 100 million tonnes worldwide. Power generation, transportation, and industrial activities account for the largest share of the total. Coal accounts for the largest share, especially in countries such as China and India, and oil and gas is the largest in the US and Europe [2]. By trapping heat in the Earth's atmosphere, these emissions cause extreme weather events, rising sea levels, and an increase in global temperatures. Furthermore, a large portion of this carbon is absorbed by the oceans, causing acidification that is detrimental to marine life. India's heavy reliance on coal and other fossil fuels makes it a major emitter of CO_2 and other greenhouse gases. It contributes roughly 7% of the world's CO_2 emissions, making it the third-largest emitter in the world, according to recent data. India's total greenhouse gas output, especially in the transportation sector, is greatly influenced by the CO_2 emissions from the use of gasoline and diesel. Together, gasoline and diesel contribute about 18–20% of India's total CO_2 emissions, according to Our World Data and the IEA. Diesel is primarily responsible for this because it powers trucks, buses, and industrial machinery. Approximately 13–14% of India's total CO_2 emissions come from diesel alone, while 5–6% come from gasoline, mostly from private vehicle use [3], [4].

With global biofuel production reaching 154 million liters annually in 2018, a 7% increase, biofuels present a promising alternative to lower CO_2 emissions. One well-known biofuel that is frequently added to gasoline is ethanol [5]. Based on the sources of production, bioethanol is divided into four generations. The most prevalent kind of bioethanol, first-generation bioethanol, is made from edible crops like corn and sugarcane. It is well-established commercially, especially in nations like the US and Brazil. Food prices rise as a result of this production method's competition with the food supply and high-water resource requirements. For instance, the demand for first-generation biofuels caused the price of oilseeds to increase by 4% and cereal prices to rise by 1% to 2% between 2000 and 2010 [6].

Bioethanol of the second generation, made from inedible feedstocks like crop waste. However, lignocellulosic biomass must first undergo a pre-treatment step in order to be broken down into its constituent lignin, cellulose, and hemicellulose, which serve as fermentation substrates. This extra step may make the process less economically viable. Enhancing pre-treatment technologies to increase effectiveness and cost-effectiveness is the main goal of current research [7]. Advanced generations, including third- and fourth-generation bioethanol, rely on algae and genetically modified organisms. Although these options require further research and investment, they hold potential for more sustainable biofuel production. Global bioethanol production in the year 2016 was approximately 100 billion litres Conversely, India alone consumed 125 billion litres of petrol and diesel cumulatively in 2020, thus, showcasing the stark imbalance in production and usage statistics of bioethanol compared to our fuel of choice [8], [9].

The production of second-generation (2G) ethanol involves several key steps, starting with the pre-treatment of lignocellulosic biomass to break down its complex structure. This is followed by enzymatic hydrolysis, where enzymes break down cellulose and hemicellulose into fermentable sugars. The sugars are then converted into ethanol through fermentation, typically using yeast or bacteria. The final step is distillation, where ethanol is separated and purified [5], [10]. Lignocellulosic agricultural waste holds significant promise as a sustainable resource for bioethanol production. While various pretreatment methods such as physical, chemical, biochemical, or hybrid are available, this study focuses on the cost-effective and efficient technique of dilute acid hydrolysis. The primary goal of pretreatment is to break down complex carbohydrates, like cellulose, into simple sugars such as glucose, facilitating their uptake by Saccharomyces cerevisiae for conversion into ethanol via biochemical metabolism.

However, the process is not without challenges. A common byproduct, furfural, forms when dilute acids, such as H_2SO_4, react with xylose, inhibiting fermentation by affecting cellular components like mitochondrial membranes and actin structures. [11], [12], [13], [14]. Calcium hydroxide improves the fermentation efficiency, by increasing the pH of the medium and thus converting furfural to furfuryl alcohol, and by providing a large surface area to adsorb furfural from the fermentation media. To test the viability of the proposed mechanism, experiments were set up with $Ca(OH)_2$ treated feedstocks. The feedstocks, such as sugarcane bagasse, apple pomace, maize husk, and rice husk, cassava peel, banana stem, cotton fibres, jack fruit peel were selected based on factors like cellulose and lignin content, availability, and cost-efficiency, making them suitable candidates for large-scale bioethanol production.

Calcium hydroxide-based pre-treatment is an established detoxification strategy for decreasing the inhibitor concentration generated during lignocellulosic hydrolysis. However, comparative investigations of ethanol productivity from calcium hydroxide pre-treated lignocellulosic feedstocks under common fermentation process conditions is limited. This study involves systematic comparison of eight locally available using same pre-treatment and fermentation operating conditions. The work integrates furfural reduction, glucose utilization, ethanol production and yeast tolerance assessment, and kinetic modelling studies to identify feedstocks with improved suitability for bioethanol production.

2. MATERIALS AND METHODS

Experimental studies were performed to determine ethanol productivity, glucose utilization and furfural concentration. All experiments were conducted in triplicate and results presented as error graphs. Error bars in graphs indicate deviation obtained from triplicate measurements.

2.1 Materials and reagents

Sugarcane Bagasse and Jackfruit Peel were obtained from local juice and fruit vendors. Apple pomace was prepared in-house after extracting juice from apples bought from local market. Cassava Peel and Banana Stem were obtained from organic kitchen waste. Maize and Rice husk were obtained from the organic agricultural waste generated by farmers. Cotton fibres waste were collected from local textile manufacturing factory. Analytical grade chemicals were used. Chemical reagents were bought from S.D. Fine Chem. Ltd., India. Yeast Extract Peptone Dextrose (YPD) Media and Saccharomyces cerevisiae were purchased from HiMedia.

2.2 Pre-Treatment and Fermentation of Lignocellulosic Feedstocks

Individual experiments were conducted with different types of feedstocks: sugarcane bagasse, apple pomace, maize husk, and rice husk, cassava peel, banana stem, cotton fibres and jack fruit peel. Each lignocellulosic biomass was first dried in a hot-air oven at 60°C and ground into a fine powder. The powder was then passed through a 40-mesh sieve to ensure uniform particle size. For acid pre-treatment, 5 g of the sieved biomass was suspended in 100 mL of 0.2 M sulfuric acid (H_2SO_4) in a 250 mL Erlenmeyer flask. The flasks were sealed with cotton plugs and incubated undisturbed at room temperature for 12 to 16 hours.

Following pre-treatment, the slurry was centrifuged at 6000 rpm for 10 minutes to remove residual solids. The supernatant was then neutralized to pH 5.0-5.5 using 1 M NaOH which is the optimal range for Saccharomyces cerevisiae fermentation. The pH-adjusted hydrolysate was autoclaved at 121°C for 15 minutes. 6 mL of each sample was withdrawn for the determination of furfural and glucose concentrations prior to inoculation. Fermentation was initiated by aseptically inoculating 6 mL of log-phase Saccharomyces cerevisiae culture (grown overnight in standard YPD broth) into the autoclaved and cooled hydrolysate. The flasks were incubated in a shaking incubator at 30°C and 120 rpm for 3 days but observations were continued for an extended period of 14 days for comparing glucose utilization, ethanol productivity and furfural reduction between the eight feedstocks. Samples were taken periodically for analysis of furfural, glucose and ethanol concentrations.

Before conducting the experiments with addition of calcium hydroxide, the $Ca(OH)_2$ concentration used was optimized based on a yeast viability assay [15], [16], [17]. The yeast survival assay was conducted by preparing a series of YPD

agar plates supplemented with increasing concentrations of $Ca(OH)_2$ (0.014 g, 0.028 g, 0.042 g, 0.056 g, 0.084 g, 0.14 g, 0.17 g, and 0.22 g). Each plate was inoculated with serially diluted yeast cultures from YPD broth (10^0 to 10^{-4} dilutions) and subsequently incubated at 30°C for one week. The assay revealed that yeast growth was inhibited at a $Ca(OH)_2$ concentration of 0.14 g, which was therefore selected for use in subsequent $Ca(OH)_2$ addition trials. At concentrations exceeding 0.14 g, a marked reduction in yeast growth was observed after three days of incubation.
In experiments involving detoxification, a modified protocol was used. After the acid-hydrolysis step, calcium hydroxide $Ca(OH)_2$ was added to the hydrolysate at a concentration of 0.14 g per gram of biomass. The mixture was incubated overnight at room temperature to allow for detoxification. Subsequently, the slurry was centrifuged, the supernatant was pH-adjusted to 5.0-5.5, autoclaved. Inoculation with Saccharomyces cerevisiae and fermentation conditions remained unchanged. Samples were taken intermittently for analysis of furfural, glucose and ethanol concentrations.

2.2 Determination of Furfural Concentration

Furfural concentrations in the pre-treated biomass hydrolysates were determined using a UV-Vis spectrophotometric method based on the protocol which utilizes the absorbance difference before and after sodium borohydride ($NaBH_4$) reduction to account for interference from acid-soluble lignin and other chromophores. Hydrolysate samples were first diluted appropriately in deionized water. A 5 mL aliquot of each diluted sample was transferred into two separate 25 mL volumetric flasks. To one flask (unreduced control), the volume was made up with deionized water and scanned using a UV-Vis spectrophotometer in the range of 200-400 nm. To the second flask, ~30 mg of $NaBH_4$ was added to reduce furfural to its corresponding alcohol. After allowing the reduction to proceed for 5 minutes, the reaction was quenched with a small amount of 3% HCl, and the volume was adjusted to 25 mL with deionized water. The absorbance of the reduced sample was then measured under the same conditions.
The absorbance difference (ΔA) between unreduced and reduced samples was calculated at 277 nm, the characteristic maximum for furfural. The concentration of furfural was calculated using the following calibration equation as derived from [18].

$$C_{furfural}(mmol/L) = 0.3156 \times \Delta A_{277} - 0.2780 \times \Delta A_{285} \quad (1)$$

2.3 Determination of Glucose Concentration

Reducing sugar concentrations in the hydrolysates were determined via the 3,5 dinitrosalicylic acid method [19]. The modified DNS reagent contained 1% (w/v) 3,5 dinitrosalicylic acid, 1% NaOH, 0.2% phenol, and 0.05% Na_2SO_3. To 0.5 mL of appropriately diluted sample, 0.5 mL of reagent was added. Reaction mixtures were boiled for 10 minutes and cooled under running water. The final volume was adjusted with distilled water, and absorbance was measured at 575 nm. Sugar concentrations were calculated by interpolation from a glucose standard curve.

2.4 Determination of Ethanol Concentration

The Ethanol concentration was determined daily using a spectrophotometric chromic acid method [20]. Chromic acid reagent was prepared by dissolving 34 g of potassium dichromate in 500 mL of distilled water, adding 325 mL of concentrated sulfuric acid, and diluting to 1 L. In each assay, 1 mL of ethanol standard or sample was diluted to 5 mL with distilled water, and 5 mL of reagent was then added. The mixture was incubated at 60 °C for 20 minutes, and absorbance was measured at 595 nm. Ethanol levels were quantified against a standard curve using varying concentrations of absolute ethanol.

2.5 Distillation of Bioethanol

At the end of the fermentation period, the broth was filtered, and the clear supernatant was subjected to distillation. Distillation was carried out at 78°C, the boiling point of ethanol, using a standard laboratory distillation apparatus. The distillate was collected in glass bottles for further downstream analysis [21].

2.7 Fourier-Transform Infrared Spectroscopy (FTIR)

FTIR spectroscopy of ethanol samples were conducted using the Thermo Fisher Scientific Nicolet instrument at Jawaharlal Nehru Centre for Advanced Scientific Research (JNCASR) in Bengaluru. The distilled ethanol samples were analysed using FTIR spectroscopy. The samples were scanned in the mid-IR region (400 to 4000 cm^{-1}). The spectra were acquired with a resolution of 4 cm^{-1}, and 64 scans were averaged for each sample to ensure that at high signal-to-noise ratio [22].

2.8 Kinetic modelling

The bioethanol production process from lignocellulose biomass involves microbial growth, ethanol formation, and substrate consumption. The present model adopts an unstructured approach in which these phenomena are described independently, without explicit consideration of intracellular mechanisms, following methodologies reported in previous fermentation studies [23].

2.8.1 Biomass growth kinetics

Microbial growth was described using the logistic equation, which is a substrate-independent model suitable for batch fermentations when growth is self-limiting due to nutrient depletion or product inhibition:

$$\frac{d[X]}{dt} = \mu_m X \left(1 - \frac{X}{X_m}\right) \quad (2)$$

where X is the biomass concentration ($g \cdot L^{-1}$), X_m is the maximum biomass concentration, and μm is the maximum specific growth rate (h^{-1}).
Integration of Eq. (2) with the initial condition $X=X_0$ at t=0 yields:

$$X(t) = \frac{X_m X_0}{X_0 + (X_m - X_0)\, e^{-\mu_m t}} \quad (3)$$

Rearrangement of Eq. (3) provides the linearized form:

$$\ln\left(\frac{X}{X - X_m}\right) = \mu_m t - \ln\left(\frac{X_m}{X_0} - 1\right) \quad (4)$$

allowing μ_m and X_0 to be estimated from the slope and intercept, respectively, using experimental biomass data.

2.8.2 Product formation kinetics

Ethanol production was described by the Luedeking–Piret model, which relates the rate of product formation to the biomass growth rate and the biomass concentration:

$$\frac{dP}{dt} = m\frac{dX}{dt} + nX \quad (5)$$

Where P is the ethanol concentration m is the growth-associated product formation constant, and n is the non-growth-associated constant.

$$P(t) = m\alpha(t) + n\beta(t) \quad (6)$$

Integration of Eq. (4) with $P = 0$ at $t = 0$ gives:

$$\alpha(t) = X_0\left[\frac{e^{-\mu_m t}}{\left(1-\left(\frac{X_m}{X_0}\right)(1-e^{-\mu_m t})\right)} - 1\right] \quad (7)$$

and

$$\beta(t) = \left(\frac{X_m}{\mu_m}\right)\ln\left(1 - \left(\frac{X_m}{X_0}\right)(1 - e^{-\mu_m t})\right) \quad (8)$$

The parameter n can be determined from the stationary phase, where $dX/dt \approx 0$, as:

$$n = \frac{(dP/dt)_{stat}}{X_m} \quad (9)$$

Subsequently, m can be estimated from the slope of a plot of P-n $\beta(t)$ versus $\alpha(t)$ and non-growth associated product formation rate constant 'n' can be determined by using Eq. (9).

3. RESULTS AND DISCUSSION

Glucose utilization, furfural concentration and ethanol yields were measured from various lignocellulose sources. Periodic measurements, which included measuring furfural concentration every two days, were done to assess the effect of calcium hydroxide on the fermentation process. Substrate sources are chosen based on their cellulose concentration. Cellulose composition for each of the substrate was determined [24]. The cellulose concentration of biomass is determined by subjecting the sample to acid hydrolysis, where concentrated sulfuric acid is initially used to disrupt the structure, followed by dilute acid treatment to hydrolyze cellulose into glucose. The released glucose is then quantified using DNS method. Finally, the glucose concentration is converted into cellulose content by applying the appropriate stoichiometric conversion factor. Table 1 shows the cellulose content estimated for various substrates and compared with the other studies.

Table 1: Cellulose content in the lignocellulosic biomass considered for the production of study: Comparison of experimental values with literature data.

Sources used	% Cellulose per 100g of dry sample	% Cellulose per 100g of dry sample as per literature
Sugarcane Bagasse	38.70±0.90	32-55 [25]
Maize Husk	31.60 ±0.26	38-40 [25]
Apple Pomace	43.60 ±0.38	36 [26]
Rice Husk	36.20±0.30	28-36 [25]
Casava Peel	44.80±1.23	40.5 [24]
Cotton Fibre	81.20±0.56	82-90 [25]
Banana Stem	48.77±0.45	48–65 [25]
Jackfruit Peel	30.00±0.32	20-23 [28]

3.1 Impact of $Ca(OH)_2$ pre-treatment on ethanol yield

Alkaline pre-treatment using calcium hydroxide $Ca(OH)_2$ is one of the cost-effective and environmentally benign option to detoxify the substrate. Comparing the fermentation yield from different sources provides insights into the impact of $Ca(OH)_2$ on ethanol concentration and the effectiveness of $Ca(OH)_2$, along with the suitability of each substrate for bioethanol production. [27]. Figures 1a and 1b illustrate the concentration of ethanol from fermentation, both before and after treatment with $Ca(OH)_2$ across various lignocellulosic sources.

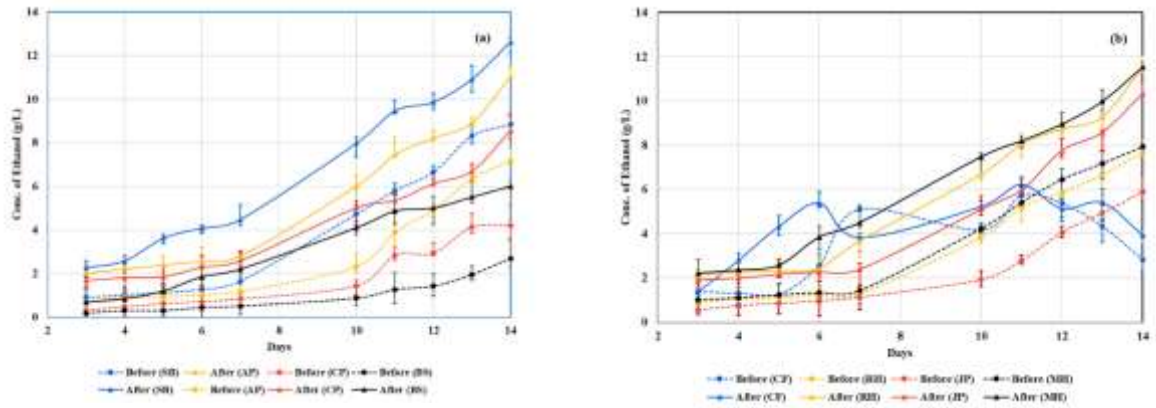

Figure 1: Effect of pretreatment of various biomass using $Ca(OH)_2$ on ethanol concentration in batch fermentation (a) before and after $Ca(OH)_2$ treatment; SB: Sugarcane Bagasse, AP: Apple Pomace, CP: Cassava Peel, BS: Banana Stem, (b) before and after $Ca(OH)_2$ treatment; CF: Cotton Fibre, RH: Rice Husk, JP: Jackfruit Peel, MH: Maize Husk

The data evidently shows that $Ca(OH)_2$ treatment increases ethanol production in all biomass kinds. This enhancement is likely due to the ability of calcium hydroxide to neutralize fermentation inhibitors, such as furfural and hydroxymethylfurfural (HMF), which otherwise hinder yeast activity during fermentation. After addition of calcium hydroxide, the highest upsurges in ethanol yield (about 2.5 to 4 g/L) were detected in all the type of biomass except cotton fibre. Sugarcane bagasse, apple pomace, banana stem and jack fruit peel showed average increase in ethanol concentration 3.5 g/L. This is due to the removal of inhibitors and more efficient conversion to ethanol. Nurhayati et al (2023) obtained 0.365 g/mL of bioethanol with refractive index of 1.35 using jackfruit straw waste [28].
Among the tested biomass sources, sugarcane bagasse (12.63 g/L), maize husk (11.54 g/ L), and rice husk (11.50 g/L) gave high ethanol concentration. These biomasses appear as the most promising types of biomasses for bioethanol production, when pre-treated with calcium hydroxide to enhance fermentation efficiency. The apparent ethanol productivity was calculated based on maximum ethanol concentration obtained at the end of fermentation. Maximum ethanol productivity was obtained from sugarcane bagasse amounting to 0.902 g/L/day, followed by maize husk (0.824 g/L/day) and rice husk (0.822 g/L/day).'

3.2 Impact of $Ca(OH)_2$ pre-treatment on Glucose Concentration

Accurate measurement of glucose concentration is crucial in assessing the efficiency of biomass hydrolysis processes, particularly in bioethanol production. Glucose acts as the main fermentable sugar, and its availability has a direct impact on fermentation performance and overall ethanol production. Factors such as the formation of inhibitory compounds, including furfural, can impact glucose release during biomass pre-treatment and enzymatic hydrolysis. Precise quantification of glucose is essential for evaluating the effectiveness of pre-treatment methods and optimizing conditions for the maximum recovery of sugar [29].

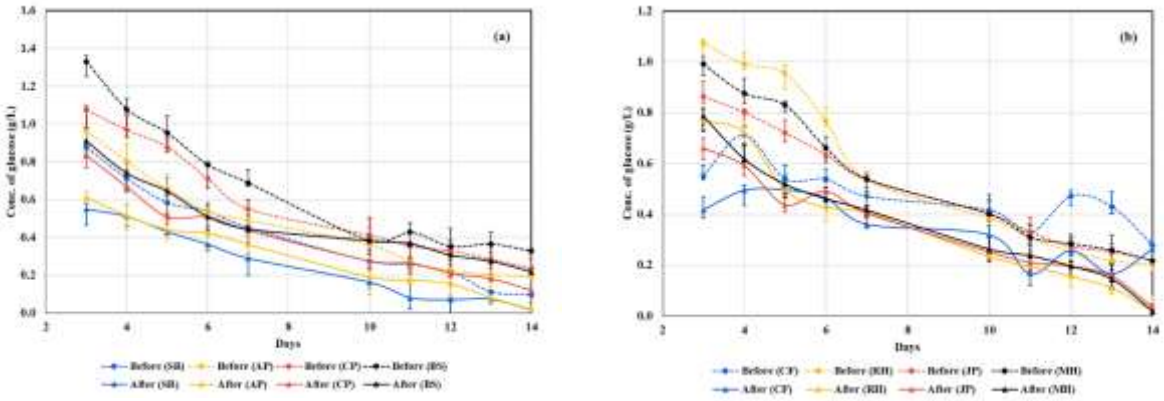

Figure 2: Effect of pretreatment of various biomass using $Ca(OH)_2$ on glucose utilization in batch fermentation: (a) before and after $Ca(OH)_2$ treatment; SB: Sugarcane Bagasse, AP: Apple Pomace, CP: Cassava Peel, BS: Banana Stem, (b) before and after $Ca(OH)_2$ treatment; CF: Cotton Fibre, RH: Rice Husk, JP: Jackfruit Peel, MH: Maize Husk

Adding $Ca(OH)_2$ helps neutralize acids that could otherwise catalyze the formation of furfural, thereby improving the overall efficiency of the bioethanol production process. However, this comes at the cost of reduced glucose availability, as observed in the graphs, where the glucose concentration significantly drops in all biomass sources after $Ca(OH)_2$ treatment. The reduction in glucose concentration after $Ca(OH)_2$ addition highlights a trade-off between furfural inhibition

and glucose availability for fermentation. While $Ca(OH)_2$ successfully inhibits furfural formation, most biomass sources show limited improvement in glucose utilization post-treatment.

After the addition of calcium hydroxide, a reduction in glucose concentration (about 0.078 to 0.126 g/L) was observed in all types of biomasses. Sugarcane bagasse, apple pumice, maize husk and jack fruit peel showed an average decrease in glucose concentration of 0.12 g/L. This corresponds to the increase in ethanol yield from the sugarcane bagasse, apple pumice, maize husk and jack fruit peel. Among the tested biomass sources, sugarcane bagasse (0.017 g/L), maize husk 0.018 g/ L), and rice husk (g/L) had the least glucose concentration at the end of fermentation. Poor glucose utilization is observed in cassava peel (0.118 g/L), banana stem (0.218 g/L) and cotton fibre (0.262 g/L).

The challenge in bioethanol production lies in maintaining a balance between suppressing inhibitors like furfural and maximizing the availability of glucose for fermentation. The addition of $Ca(OH)_2$ effectively reduces furfural but at the cost of hydrolysis efficiency, resulting in lower glucose utilization. Therefore, it is crucial to optimize the $Ca(OH)_2$ concentration or combine it with other pre-treatment techniques that can selectively inhibit furfural while preserving or even enhancing glucose availability.

3.3 Influence of $Ca(OH)_2$ pre-treatment on furfural suppression

Lignocellulosic biomass is a renewable feedstock that provides an abundant source of material for the production of bioethanol; however, pre-treatment may produce fermentation inhibitors (e.g., furfural), which inhibit microbial growth and decrease ethanol yields. Therefore, detoxification steps are important to improve the efficiency of processes used to produce bioethanol [30], [31]. The addition of calcium hydroxide $Ca(OH)_2$ has been found to neutralize inhibitory compounds; therefore, we examine the effect on furfural concentrations in several biomass sources that could be suitable for fermentation-based ethanol production [32].

Table 2 show the furfural concentrations, a known inhibitor of microbial fermentation, in various biomass sources both before and after adding calcium hydroxide $Ca(OH)_2$. Furfural is a byproduct of lignocellulosic biomass breakdown and can significantly slow down bioethanol production by hindering the activity of yeast and other microorganisms involved in fermentation [18]**.** During the fermentation of lignocellulosic hydrolysates, calcium hydroxide $Ca(OH)_2$ is essential for increasing yeast biomass and ethanol production because it detoxifies inhibitory chemicals, especially furfural and 5-hydroxymethylfurfural (HMF). These furans which are produced during the acid hydrolysis of cellulose and hemicellulose suppress yeast metabolism by interfering with enzyme function, causing cellular damage and oxidative stress. Through alkaline-mediated reactions, the addition of $Ca(OH)_2$ promotes the chemical conversion of furfural and HMF into less hazardous substances such as furoic acids or inert polymeric forms. The hydrolysate's acidity is neutralized as part of this detoxification process, resulting in a pH environment (usually between 5.0 and 6.0) that is ideal for Saccharomyces cerevisiae growth and enzymatic activity. Higher yeast viability, rapid biomass growth, and more effective fermentation are all encouraged by the better circumstances. Furthermore, phenolic chemicals and organic acids can be precipitated or adsorbed by calcium ions, which lowers the medium's total inhibitor load. Also, by deacetylating hemicellulosic oligomers, mild alkaline treatment can improve the release and availability of fermentable sugars, hence improving substrate accessibility [30], [32].

Table 2: Furfural Concentration comparison before and after treatment with $Ca(OH)_2$

Sources used	Furfural concentration		% Reduction in Furfural
	Without $Ca(OH)_2$ addition (mg/L)	With $Ca(OH)_2$ addition (mg/L)	
Sugarcane Bagasse	1.77 ±0.001	0.53 ±0.03	70.2
Maize Husk	1.80 ±0.011	0.71 ±0.015	60.7
Apple Pomace	2.22 ±0.002	0.55 ±0.033	75.4
Rice Husk	1.42 ±0.006	0.82 ±0.015	42.5
Casava Peel	0.82 ±0.011	0.44 ±0.032	46.4
Cotton Fibre	4.10 ±0.071	3.31 ±0.096	19.2
Banana Stem	0.61 ±0.018	0.36 ±0.079	40.7
Jackfruit Peel	2.14±0.004	0.42±0.033	80.4

According to the data, $Ca(OH)_2$ addition effectively reduces the furfural concentration in all samples, enhancing the fermentation conditions and ethanol yields. Significant decrease in furfural concentrations was observed with treating sugarcane bagasse and jackfruit peel with $Ca(OH)_2$. Due to the reduced inhibitor concentration, yeast and other microorganisms were able to ferment more [33]. A median decrease in furfural concentrations was recorded with maize husk and apple pomace, where even after starting with a high furfural concentration, significant reductions were observed, making them a viable option for bioethanol production as well. However, they still retain a slightly higher amount of furfural concentrations compared to other sources [34].

Rice husk, despite starting with moderate furfural levels, retains relatively high amounts (0.817mg/L) even after detoxification. This implies that in order to achieve the best conditions for fermentation, rice husk may require additional or more thorough detoxification [35]**.** All biomass sources, including sugarcane bagasse and jackfruit peel responded with decreases furfural concentration to the $Ca(OH)_2$ treatment, which makes them promising candidates for bioethanol production. The comparative observations made are consolidated in Table 3 for all the eight feedstocks.

Table 3: Comparison of Ethanol productivity and glucose utilization among the eight lignocellulosic feedstocks

Feedstock	Final Ethanol concentration (g/L)	Ethanol productivity (g/L/day)	Initial Glucose (g/L)	Final Glucose (g/L)	Glucose utilization (%)
Sugarcane Bagasse	12.634	0.902	0.879	0.017	98.1
Apple Pomace	11.027	0.788	0.964	0.020	97.9
Cassava Peel	8.572	0.612	1.074	0.118	89.0
Banana Stem	6.012	0.429	1.331	0.218	83.6
Maize Husk	11.541	0.824	0.991	0.018	98.2
Jackfruit Peel	10.333	0.738	0.863	0.035	95.9
Rice Husk	11.503	0.822	1.074	0.021	98.0
Cotton Fibres	3.945	0.282	0.551	0.262	52.5

3.4 Qualitative Analysis of Bioethanol

Fourier Transform Infrared (FTIR) spectroscopy is a technique that compares the FTIR spectra of the produced samples against ethanol standards and helps in determining qualitatively the presence of bioethanol obtained from various sources. The following section illustrates FTIR analysis for validating the chemical structure of ethanol derived from pretreated and fermented biomass and to obtain insights into the efficiency of the fermentation and distillation processes by deducing the relative purity of each sample based on the intensity and sharpness of the peak obtained.

The FTIR spectra of bioethanol samples derived from various biomass sources are shown in Figure 3. This spectral analysis helps identify characteristic functional groups, verify the presence of ethanol associated functional groups, and detect possible impurities resulting from fermentation or oxidative degradation [36].

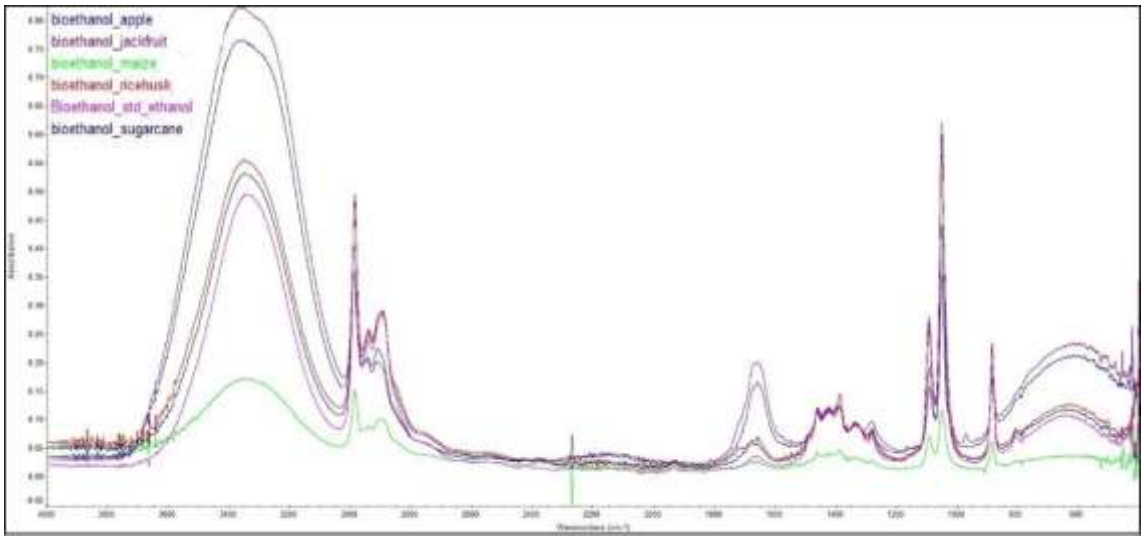

Figure 3: FTIR Spectra of functional groups associated with bioethanol samples produced using sources: apple pomace, jackfruit peel, maize husk, rice husk, sugarcane bagasse. The spectrum was compared with spectrum of standard ethanol sample shown in violet color.

A broad and intense absorbance peak was consistently observed in the region between 3200 and 3550 cm^{-1} across all bioethanol samples, as well as the standard ethanol. This peak is characteristic of hydroxyl groups, corresponding to the O–H stretching vibration. The broad shape indicates hydrogen bonding, which is common in ethanol [37]. The increased peak intensity and broadening of the shapes indicate the presence of extra hydroxyl groups such as polyols, unfermented sugars or leftover fermentation intermediates [34], [38]. There were several peaks in the 2850–3000 cm^{-1} range, which were ascribed to the stretching vibrations of the C–H bonds in alkyl chains. Verified the structural integrity of ethanol and preservation of the alkyl groups from all sources, including the standard ethanol [39]. Minor intensity differences may be linked to variations in ethanol concentration among the samples.

A weak absorbance peak might show up in the area around 1700–1750 cm^{-1}, which could be a sign of the presence of impurities that contain carbonyls, like leftover acetaldehyde. The absence of these peaks in the standard ethanol sample indicates that these might be from impurities in the fermentation broth or oxidation products obtained in the process. The notable peaks between 1000 and 1300 cm^{-1}, which are associated with O-H bending and C-O stretching vibrations, are

observed in all the samples, including the standard. This region is crucial for the identification of ethanol and is termed as the fingerprint region [40]. Peak intensity fluctuations, however, point to variations in sample composition; it is probable that some batches of bioethanol contain extra organic compounds from the fermentation matrix or biomass residues [41]. Absorption peaks in the region of 1350–1480 cm^{-1}, attributed to C–H bending vibrations in alkyl groups, were also consistently present. These peaks indicate that the alkyl group composition of ethanol remains consistent across various sources. Small variations in the peak intensity reflect the minor differences in the chemical environment or concentration of ethanol [39].

The increased O-H bond stretching is due to the increase in hydrogen bonding, which could be due to leftover fermentation products such as organic acids or unreacted carbohydrates [34], [42]. A slightly higher C-O stretching and a decreased intensity of C-H can be attributed to the leftover trace amounts of carbonyl impurities and dilution or degradation of ethanol, respectively [42]. FTIR analysis confirms the presence of ethanol-associated functional groups in every sample [43], [44]. However, since FTIR alone cannot be used to determine ethanol purity and its quantification, therefore, the present analysis is restricted to qualitative confirmation of functional groups associated with ethanol rather than purity assessment.

3.5 Mathematical model to predict the yield of ethanol

Bioethanol production kinetics can be described using the Luedeking–Piret model, which relates product formation to microbial growth. According to this model, it is possible to determine if ethanol generation occurs through growth-associated and non-growth-associated pathways, or both. In this study, bioethanol production followed Luedeking- Piret model. The kinetic parameters were calculated by using Equation (6) at stationary phase (dX/dt = 0) where 'm' is the growth associated rate constant and 'n' is the non-growth associated rate constant. The bioethanol production in this study had good agreement with the experimental results of substrate Sugarcane Bagasse, Apple Pomace Maize Husk, Jackfruit Peel as shown in Figure 4. The reasons for slight variations in the results may be due to the microorganisms used and the environmental conditions for bioethanol production. The growth associated rate constant 'm' is zero for all the sources and non-growth associated rate constant 'n' were obtained as 0.009928, 0.007728, 0.009006, 0.006845 $Ug_{biomass}^{-1}h^{-1}$ respectively. These results showed that the non-growth associated rate constant 'n' is active. If the growth-associated rate constant 'm' is zero, it means that the production of ethanol predominantly suggests non-growth-associated for the experimental conditions employed for the study. Essentially, this means that ethanol is generated solely during the maintenance phase of the microorganism. This implies that the process of ethanol synthesis is not directly linked to cell division or the accumulation of biomass; instead, it mainly happens when the cells are metabolically active but not increasing in number, which is known as the stationary phase. Additionally, the interpretations are model dependent and the parameter reliability maybe influenced by variations in sampling frequency, biomass measurements and experimental procedures. Therefore, future studies including additional kinetic parameters and advanced modeling approaches are recommended for validation.

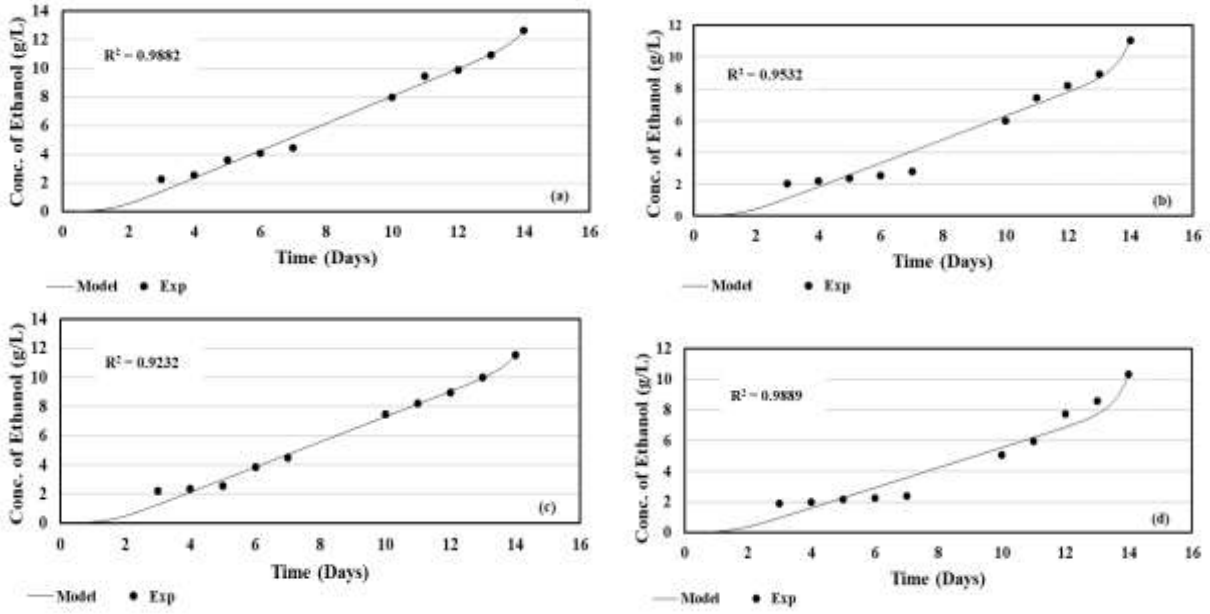

Figure 4: Comparison of time course profile for experimental and predicted data using mathematical model of ethanol concentration in batch fermentation: (a) Sugarcane Bagasse, (b) Apple Pomace, (c) Maize Husk, (d) Jackfruit peel

4. CONCLUSIONS

This study provides critical insights into improving bioethanol production from lignocellulosic and agricultural residues by addressing the challenges posed by fermentation inhibitors produced during dilute acid pre-treatment. Calcium hydroxide detoxification strategy was found to be efficient in most of the feedstocks by reducing furfural concentration and increasing glucose utilization. Among all the feed substrates, sugarcane bagasse, maize husk and rice husk showed

relatively higher ethanol production under laboratory scale operating conditions. FTIR analysis qualitatively confirmed the presence of ethanol associated functional groups and kinetic studies through mathematical modelling indicated predominantly non-growth associated ethanol production. Though calcium hydroxide detoxification was found to be effective in reducing furfural concentrations in all the lignocellulosic feedstocks, several further studies need to be conducted before industrial implementation. Extended fermentation duration can impact ethanol productivity on a larger scale. Further, centrifugation-based separation, pH adjustments, lime sludge formation, and feedstock properties can affect scalability and process economics. Therefore, further studies must be conducted on optimization focusing on feedstock hydrolysis efficiency, shorter fermentation durations, simultaneous saccharifications along with solid state fermentation, fed-batch operations and quantification and purity assessment of the ethanol produced through advance chromatographic techniques.

Declaration

The authors declare that no ethical approval was required for this study. The authors declare no conflict of interest.

Data availability

The datasets used and/or analyzed during the current study available from the corresponding author on reasonable request.

Funding

No financial assistance was provided in this work.

Authors Contributions

Praphulla Rao contributed to the planning, designing and execution of the experiments result compilation and manuscript preparation. Prathibha Narayanan contributed to providing inputs for execution of project and preparing and reviewing the manuscript. Tarun Mahesh, P Abhi Ram and Chandu R contributed to the execution of experiments and manuscript preparation. Rohith Vasishta J and Hadagali Ashoka contributed to manuscript preparation.

Acknowledgements

All the authors thank Management and Principal of B.M.S College of Engineering, Bengaluru to carry out this research work.

REFERENCES

[1] Huang, Z., & Ren, X., Impact of natural resources, resilient economic growth, and energy consumption on CO_2 emissions. Resour. Policy, **90,** 104714 (2024).
[2] Friedlingstein, P.et al., Global Carbon Budget 2024. Earth Syst. Sci. Data, **17(2),** 965–982 (2025).
[3] World Energy Outlook https://www.iea.org/reports/india-energy-outlook-2023 (2023).
[4] Ritchie, H., & Roser, M., CO_2 and greenhouse gas emissions. Our World in Data. https://ourworldindata.org/co2-and-other-greenhouse-gas-emissions. (2023).
[5] Tse, T. J., Wiens, D. J., & Reaney, M. J. T, Production of bioethanol—A review of factors affecting ethanol yield. Fermentation. **7(4),** 268 (2021).
[6] Janda, K., Michalikova, E., Rocha, L. C. S., Rotella Junior, P., Schererova, B., & Zilberman, D., Review of the Impact of Biofuels on U.S. Retail Gasoline Prices. Energies, **16(1),** 428 (2023).
[7] Shukla, A. et al., Strategies of pretreatment of feedstocks for optimized bioethanol production: Distinct and integrated approaches. Biotechnol. Biofuels and Bioproducts, **16**, 44 (2023).
[8] Inter-American Institute for Cooperation on Agriculture (IICA). Liquid Biofuels Atlas 2023–2024. Retrieved from https://iica.int/en/news/with-global-production-growing-by-50-over-the-past-decade-liquid-biofuels-continue-to-consolidate-their-position-as-a-key-tool-for-the-energy-transition-reveals-the-latest-edition-of-the-iica-atlas/ (2024).
[9] Statista. Fuel market consumption volume in India from 2011 to 2020 (in billion liters). Energy & Environment Retrieved from https://www.statista.com/statistics/1051895/india-consumption-volume-fuel-market/ (2020).
[10] Pathak, N et al. Valorization of jackfruit waste into value-added products and their potential applications. Front. Nutr., **9**, 1061098 (2022).
[11] Kausar, F. et al., Challenges in bioethanol production: Effect of inhibitory compounds. Bioenergy Research: Basic and Advanced Concepts. Clean Energy Production Technologies. Springer, Singapore (pp. 119–154). Springer. https://doi.org/10.1007/978-981-33-4611-6_5 (2021).
[12] Field, S. J., et al., Identification of furfural resistant strains of Saccharomyces cerevisiae and Saccharomyces paradoxus from a collection of environmental and industrial isolates. Biotechnol. Biofuels, **8(1)**, (2015).
[13] Allen, S. A et al., Furfural induces reactive oxygen species accumulation and cellular damage in Saccharomyces cerevisiae. Biotechnol. Biofuels, **3**, 2. https://doi.org/10.1186/1754-6834-3-2 (2010).
[14] Hyunjoo Park, E., Kim, E., Jun, T., Pyo, S.-H., & Kim, S.-H, Colorimetric detection of furfural with enhanced visible absorption of furfural-DNPH in basic conditions. ACS Omega, **9(2),** 2519–2527. (2024).
[15] Xu, X., Lambrecht, A. D., & Xiao, W., Yeast survival and growth assays. In Methods in Molecular Biology. **1163**, pp. 183–191). https://doi.org/10.1007/978-1-4939-0799-1_13 (2014).
[16] Sierra, R., Granda, C., & Holtzapple, M. Lime pretreatment. Mielenz, J. (eds) Biofuels. Methods in Molecular Biology, **581**, 115–124. https://doi.org/10.1007/978-1-60761-214-8_9 (2009).
[17] Lee, I., & Yu, J.-H., Design of hydrothermal and subsequent lime pretreatment for fermentable sugar and bioethanol production from Acacia wood. Renew. Energy, **174**, 170–177. (2021).

[18] Chi, C., Zhang, Z., Chang, H., & Jameel, H., Determination of furfural and hydroxymethylfurfural formed from biomass under acidic conditions. J. Wood Chem. Technol., **29(4),** 265–276. https://doi.org/10.1080/02773810903096025 (2009).
[19] Miller, G. L. Use of dinitrosalicylic acid reagent for determination of reducing sugar. Anal. Chem., **31,** 426–428. (1959).
[20] Caputi, A., Ueda, M., & Brown, T. Spectrophotometric determination of ethanol in wine. Am. J. Enol. Vitic., **19(3),** 160–165. (1968).
[21] Gani, M., Abdulkadir, N., Usman, S. B., Maiturare, H. M., & Gabriel, S. Production of bioethanol from sugarcane bagasse using Saccharomyces cerevisiae. Biotechnol. J. Int., **22(1).** (2018).
[22] Luis, F. et al., Application of Fourier transform infrared spectroscopy (FTIR) techniques in the mid-IR (MIR) and near-IR (NIR) spectroscopy to determine n-alkane and long-chain alcohol contents in plant species and faecal samples. Spectrochim. Acta A Mol. Biomol. Spectrosc., **280**, 121544. (2022).
[23] Vinayagam R, Vytla RM and Chandrasekaran M. Development of a Simple Kinetic Model and Parameter Estimation for Biomass and Nattokinase Production by Bacillus subtilis 1A752. Austin J Biotechnol Bioeng.;**2(1),** 1036. (2015).
[24] Widiarto, S., Pramono, E., Suharso, Rochliadi, A., & Arcana, I. M. Cellulose nanofibers preparation from cassava peels via mechanical disruption. Fibers, **7(5),** 44. https://doi.org/10.3390/fib7050044 (2019).
[25] Lozada, R. E., Gutiérrez Aguilar, C. M., Jaramillo Carvalho, J. A., Sánchez, J. C., & Barrera Torres, G. Vegetable cellulose fibers in natural rubber composites. Polymers, **15(13),** 2914. https://doi.org/10.3390/polym15132914 (2023).
[26] Pathania, S., Sharma, N., & Handa, S. Utilization of horticultural waste (apple pomace) for multiple carbohydrase production from Rhizopus delemar F2 under solid state fermentation. J. Genet. Eng. Biotechnol., **15(2),** 239-245. https://doi.org/10.1016/j.jgeb.2017.10.013 (2017).
[27] Yu, J., Chen, S., Yu, Y., Zhang, C., & Jin, M. Influence of feedstock selection on cellulosic ethanol production based on densified biomass with calcium hydroxide and regular steam pretreatment. Renew. Energy, **227**, Article 120561. (2024).
[28] Nurhayati, I., Aisyah, I., Sundari, C. D. D., Rahmawati, R. R., & Suryaningsih, S. Optimization of bioethanol production from jackfruit straw waste through the addition of a starter and fermentation duration. AIP Conf. Proc., **2572**, 030014. (2023).
[29] Megawati, M., Bahlawan, Z. A. S., Damayanti, A., Putri, R. D. A., Triwibowo, B., & Prasetiawan, H. Comparative Study on the Various Hydrolysis and Fermentation Methods of Chlorella vulgaris Biomass for the Production of Bioethanol. International Journal of Renew. Energy Development, **11(2),** 515-522. https://doi.org/10.14710/ijred.2022.41696. (2022).
[30] Palmqvist, E., & Hahn-Hägerdal, B. Fermentation of lignocellulosic hydrolysates. I: Inhibition and detoxification. Bioresour. Technol., **74(1),** 17–24. (2000).
[31] Guo, H., Zhao, Y., Chang, J. S., & Lee, D. J. Inhibitor formation and detoxification during lignocellulose biorefinery: A review. Bioresource technology, **361**, 127666. https://doi.org/10.1016/j.biortech.2022.127666 (2022).
[32] Martinez, A., Rodriguez, M.E., York, S.W., Preston, J.F. and Ingram, L.O. Effects of Ca(OH)2 treatments ("overliming") on the composition and toxicity of bagasse hemicellulose hydrolysates. Biotechnol. Bioeng., **69,** 526-536. https://doi.org/10.1002/1097-0290(20000905)69:5<526::AID-BIT7>3.0.CO;2-E (2000).
[33] Chandel, A. K., et al. Detoxification of lignocellulosic hydrolysates for improved bioethanol production. Biofuel Production-Recent Developments and Prospects. InTech. (2011).
[34] Mussatto, S. I., et al. Technological trends, global market, and challenges of bio-ethanol production. Biotechnology Advances, **28(6),** 817-830. (2010).
[35] Alvira, P., Tomás-Pejó, E., Ballesteros, M., & Negro, M. J. Pretreatment technologies for an efficient bioethanol production process based on enzymatic hydrolysis: A review. Bioresour. Technol., **101(13),** 4851–4861. (2010).
[36] Sánchez, Ó. J., & Cardona, C. A. Trends in biotechnological production of fuel ethanol from different feedstocks Bioresour. Technol., **99(13),** 5270–5295. (2008).
[37] Smith, B. C. Fundamentals of Fourier Transform Infrared Spectroscopy. CRC Press. (2011).
[38] Taherzadeh, M. J., & Karimi, K. Acid-Based Hydrolysis Processes For Ethanol From Lignocellulosic Materials: A Review Bioresour., **2(3),** 472–499. (2007).
[39] Coates, J. Interpretation of infrared spectra: A practical approach. In R. A. Meyers (Ed.), Encyclopedia of Anal. Chem. (pp. 10815–10837). John Wiley & Sons. (2000).
[40] Stuart, B. Infrared Spectroscopy: Fundamentals and Applications. John Wiley & Sons. (2004).
[41] Buranov, A. U., & Mazza, G. Lignin in straw of herbaceous crops. Ind. Crops Prod., **28(3),** 237–259. (2008).
[42] Limayem, A., & Ricke, S. C. Lignocellulosic biomass for bioethanol production: Current perspectives, potential issues and future prospects Prog. Energy Combust. Sci., **38(4),** 449–467. (2012).
[43] Balat, M., Balat, H., & Öz, C. Progress in bioethanol processing. Prog. Energy Combust. Sci., **34(5),** 551–573. (2008).
[44] Demirbas, A. Energy Sources, Part A: Recovery, Util. Environ. Eff., **31(14),** 1245–1252. (2009).